

# Can R CrB stars form from the merger of two helium white dwarfs?

Xianfei Zhang<sup>1\*</sup> and C. Simon Jeffery<sup>1,2†</sup>

<sup>1</sup>*Armagh Observatory, College Hill, Armagh BT61 9DG, UK*

<sup>2</sup>*School of Physics, Trinity College Dublin, Dublin 2, Ireland*

Accepted . Received ; in original form

## ABSTRACT

Due to orbital decay by gravitational-wave radiation, some close-binary helium white dwarfs are expected to merge within a Hubble time. The immediate merger products are believed to be helium-rich sdO stars, essentially helium main-sequence stars. We present new evolution calculations for these post-merger stars beyond the core helium-burning phase. The most massive He-sdO's develop a strong helium-burning shell and evolve to become helium-rich giants. We include nucleosynthesis calculations following the merger of  $0.4M_{\odot}$  helium white-dwarf pairs with metallicities  $Z = 0.0001, 0.004, 0.008$  and  $0.02$ . The surface chemistries of the resulting giants are in partial agreement with the observed abundances of R Coronae Borealis and extreme helium stars. Such stars might represent a third, albeit rare, evolution channel for the latter, in addition to the CO+He white dwarf merger and the very-late thermal pulse channels proposed previously. We confirm a recent suggestion that lithium seen in R CrB stars could form naturally during the hot phase of a merger in the presence of  ${}^3\text{He}$  from the donor white dwarf.

**Key words:** stars: peculiar (helium), stars: evolution, stars: white dwarfs, stars: abundances, binaries: close

## 1 INTRODUCTION

The existence of close binary white dwarfs has been predicted theoretically (Han 1998; Nelemans et al. 2000, 2001) and demonstrated observationally (Rebassa-Mansergas et al. 2011; Brown et al. 2011; Kilic et al. 2010, 2011). It has been demonstrated that the orbits of close binaries decay through the emission of gravitational wave radiation (Evans et al. 1987; Cropper et al. 1998). Models for the merger of nearly-equal mass white dwarfs following spiral-in demonstrate that these occur on a dynamical timescale (minutes) (Benz et al. 1990; Guerrero et al. 2004; Pakmor et al. 2011). The less massive WD is disrupted and part of the debris forms a prompt hot corona, the remainder forms a disk which subsequently accretes onto the surviving white dwarf (Yoon et al. 2007; Lorén-Aguilar et al. 2009). Models for the evolution of the product of a double helium-white-dwarf merger demonstrate the off-centre ignition of helium burning, followed by expansion and evolution onto the helium main sequence (Saio & Jeffery 2000). Models which include the composite nature of the debris (corona + disk) successfully account for the distribution in effective tempera-

ture, luminosity and surface composition of compact helium-rich subdwarf O stars (Zhang & Jeffery 2012). In particular, the most-massive mergers become the hottest sdO stars with carbon-rich surfaces, whilst the least-massive mergers are cooler with predominantly nitrogen-rich surfaces.

Following inward migration of the helium-burning shell, the merged star is essentially a helium main-sequence star having a mass between  $0.4$  and  $1.0 M_{\odot}$ , although its surface layers will carry a record of the merger event. The evolution of low-mass helium stars has been studied for over 40 years (Paczynski 1971; Dinger 1972; Trimble & Paczynski 1973; Weiss 1987). The lowest-mass stars will evolve directly to become CO/He white dwarfs following core helium exhaustion. For  $M \geq 1.0M_{\odot}$ , shell helium burning will ignite around the carbon/oxygen core, and the star will expand to become a giant. Early authors proposed this as a possible origin for the hydrogen-deficient R Coronae Borealis (R CrB) variables (Paczynski 1971; Weiss 1987).

R CrB stars and the hotter extreme helium stars are low-mass supergiants of spectral types F, A and B. Their surfaces are extremely deficient in hydrogen, and enriched in carbon, oxygen, neon and other nuclear waste. Two principle evolution channels have been established. A small fraction may be produced following a late thermal pulse in a post-asymptotic giant-branch star on the white dwarf cool-

\* E-mail: xiz@arm.ac.uk

† E-mail: csj@arm.ac.uk

ing sequence (Iben & Renzini 1984; Clayton et al. 2011). The majority are more likely to have been produced following the merger of a carbon-oxygen white dwarf with a helium white dwarf (Webbink 1984; Saio & Jeffery 2002; Jeffery et al. 2011; Longland et al. 2011).

In this letter we demonstrate that high-mass double helium-white-dwarf mergers could contribute a third evolution channel and account for some, at least, of the lowest luminosity R CrB and extreme helium stars.

## 2 MODELS

### 2.1 Evolution

Numerical simulations of stellar evolution are carried out using the stellar-evolution code "Modules for Experiments in Stellar Astrophysics" (MESA) (Paxton et al. 2011). Helium-white-dwarf models were generated by evolving a  $2 M_{\odot}$  main sequence star and removing the envelope when this reached the required mass (see Zhang & Jeffery (2012) for details). The post-merger evolution was modelled by considering fast accretion at  $10^4 M_{\odot} \text{yr}^{-1}$  (representing the formation of a hot corona), followed by slow accretion at  $10^{-5} M_{\odot} \text{yr}^{-1}$  (representing accretion from a Keplerian disk). Zhang & Jeffery (2012) considered three sets of assumptions concerning this accretion: i) all fast, ii) all slow, and iii) composite. In the composite model, most of the mass of the donor white dwarf is ingested into the hot corona, with  $0.1 M_{\odot}$  remaining in the Keplerian disk for slow accretion.

The evolution from off-center helium ignition to the end of core helium burning has been discussed and compared favourably with observations of helium-rich subdwarf B and O stars (Zhang & Jeffery 2012). Following core helium exhaustion, the post-merger models with  $M = 0.5, 0.6$  and  $0.7 M_{\odot}$  developed a brief phase of thick helium shell burning, before helium burning ends and the stars contract to become CO/He white dwarfs. The models with  $M = 0.8 M_{\odot}$  ( $M_{\text{core}} = 0.64 M_{\odot}$ ) developed a thin helium-burning shell and evolved to high luminosity and low effective temperature. This is a regime occupied by another class of hydrogen-deficient star, the R CrB stars.

We have made additional calculations for these  $0.4+0.4 M_{\odot}$  mergers with metallicities  $Z = 0.0001, 0.004, 0.008$  and  $0.02$  to investigate whether the He+He WD merger channel could produce some of the observed EHe and R CrB stars.

### 2.2 Nucleosynthesis

In the SPH simulations of white dwarf mergers, matter in the hot coronae may briefly reach temperatures of  $6 \times 10^8 \text{K}$  or more (Yoon et al. 2007; Lorén-Aguilar et al. 2009), so that some nucleosynthesis of  $\alpha$ -rich material will occur. Similarly, our one-dimensional quasi-equilibrium calculations indicate coronal temperatures up to  $4 \times 10^8 \text{K}$  for a  $0.4+0.4 M_{\odot}$  merger (Zhang & Jeffery 2012). At these temperatures, the  $3\alpha$  and other alpha capture reactions are ignited at the surface of the accretor almost immediately. Thus, carbon is produced by helium burning and nitrogen is destroyed by  $\alpha$  capture. As Warner (1967) and Clayton et al. (2007) indicated, the destruction of  $^{14}\text{N}$  by the  $^{14}\text{N}(\alpha, \gamma)^{18}\text{O}$  reaction becomes more efficient than it is at low temperature. As

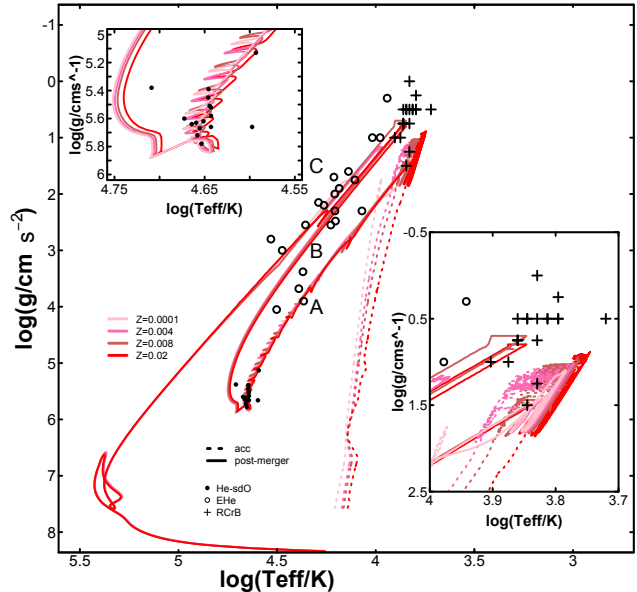


**Figure 1.** Evolutionary tracks at different metallicities on a surface gravity – effective temperature diagram for a  $0.8 M_{\odot}$  post-merger model for a He+He white-dwarf binary. The dashed line shows the evolution track during accretion, solid lines show the post-merger evolution. The colour from grey to dark (a colour version is available in the online journal, from pink to red) shows the different metallicities, i.e.  $Z = 0.0001, 0.004, 0.008, 0.02$ . The cross symbols shows the R CrB stars from Jeffery et al. (2011), the circle symbols shows the EHe stars from Jeffery et al. (2011), the dots show the He-sdO stars from Hirsch (2009). The inset top left shows an enlargement around the phase of core helium burning. The inset lower right shows an enlargement of the R CrB star region. Three stages are marked: A for inward shell-burning; B for outward shell-burning; C for giant branch to white dwarf.

the temperature continues to increase,  $^{18}\text{O}$  produces  $^{22}\text{Ne}$  through  $\alpha$  capturing. The question is whether the composition of these surface layers also matches that of the R CrB stars.

## 3 RESULTS

### 3.1 Evolution tracks

Taking the  $Z = 0.02$  model as an example, during the fast accretion stage a hot corona with a radius of  $0.06 R_{\odot}$  is formed within 16 minutes, whilst the luminosity ( $\log L/L_{\odot}$ ) increases from  $-2$  to  $-1$ . As the fast accretion starts, the coronal temperature reaches  $10^8 \text{K}$  very quickly. At the end of the fast phase, the helium-burning shell reaches a peak temperature of about  $4 \times 10^8 \text{K}$ . During this process, an almost completely convective envelope is produced due to the corona being heated by the energy produced by helium burning.

After the fast merger phase, the remaining mass of the secondary forms a Keplerian disc surrounding the accretor and transfers mass to the central object at a rate comparable to the Eddington accretion rate. During this slow-accretion phase, the helium-burning shell still heats the corona, forcing it to continue expanding. Thus, the star expands to

$\approx 32 R_{\odot}$  within  $4 \times 10^3$  yrs and then contracts away from the giant branch (Fig. 1).

During subsequent evolution, there follow about 20 helium flashes in  $6 \times 10^5$  yrs, each subsequent flash decreasing in intensity, until the helium-burning shell (flame) reaches the centre of the star. This corresponds to the end of the loops on the  $g - T_{\text{eff}}$  diagram. After this, a standard core-helium burning phase is established, followed by a normal helium-shell burning phase, leading to higher luminosity, and finally cooling to the white dwarf sequence. Just before reaching the white dwarf sequence, there is a small loop caused by a weak final helium shell flash (Fig. 1).

In order to compare with observations, data for 13 R CrB stars and 21 EHe stars are taken from Jeffery et al. (2011) and for 15 He-sdO stars from Hirsch (2009). As Fig. 1 shows, most of the EHe and R CrB stars lie around the low-gravity evolution corresponding to outward shell-helium burning after core-helium burning. Four or five of the EHe stars lie closer to the high-gravity inward shell-burning phase. After this phase they evolve to become He-sdO stars as Saio & Jeffery (2000) indicated. Two R CrB stars (RT Nor and RS Tel) have high enough gravities to be immediate post-merger objects. They may still have a disc surrounding them or be surrounded by dust. Thus, there is a channel from the He+He white dwarf merger which can produce R CrB stars, then possibly EHe stars, and then He-sdO stars. Subsequently, massive He-sdO stars might evolve to become EHe and R CrB stars once again, before finally cooling to become white dwarfs. We note that this channel will not generate metal-poor R CrB stars, due to lower opacity in the stellar envelope, but can generate low-metallicity EHe stars (e.g. BD+10 2179; Kupfer et al. 2012).

### 3.2 Surface composition

At the beginning of the fast-accretion phase, the corona is fully convective, and helium burning makes the corona rich in  $^{12}\text{C}$ ,  $^{18}\text{O}$  and  $^{22}\text{Ne}$ . At the end of fast accretion and beginning of slow accretion, flash-driven convection mixes  $^{12}\text{C}$  throughout the  $0.3 M_{\odot}$  envelope. Although this material is subsequently buried by C-poor material from the disk, the deep opacity-driven convection which follows each shell-pulse dredges carbon-rich material to the new surface, so that the final product, after slow-accretion terminates, is rich in  $^{12}\text{C}$  and  $^{22}\text{Ne}$ .

The most recent measurements of the surface abundances of EHe and R CrB stars have been collated by Jeffery et al. (2011). Here we summarise the main observational features and compare these with our results; see Fig. 2 for details.

**Carbon** is enriched in all EHe and R CrB stars. Excluding MV Sgr, the EHe stars show a mean carbon abundance  $\log \epsilon = 9.3$ , and a range from 8.9–9.7. The carbon abundance is more difficult to measure in R CrBs. Furthermore, in R CrB stars cool enough to show CO, the  $^{12}\text{C}/^{13}\text{C}$  ratios are very large (500), indicating a  $3\alpha$  or helium-burning origin for the carbon excess. In our models, the  $^{12}\text{C}$  was produced by helium burning through  $3\alpha$  reaction during the hot accretion phase, and then brought up to the surface during the slow-accretion phase by flash-driven convection. The  $^{13}\text{C}$  abundance remained almost unchanged during the whole simu-

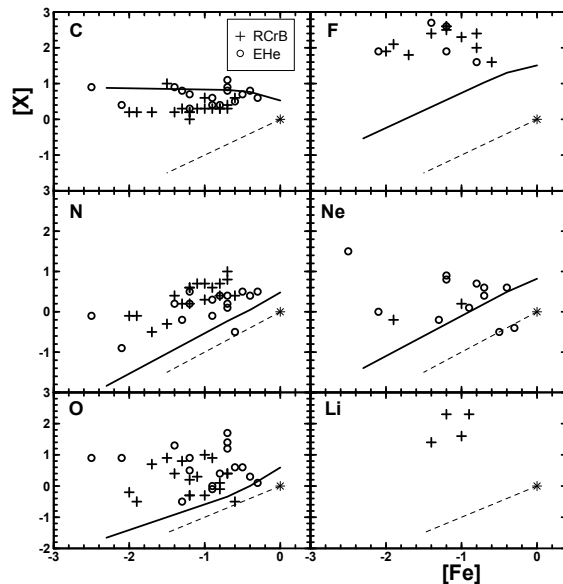


**Figure 2.** The observed surface abundances of R CrB and EHe stars (Jeffery et al. 2011) compared with our nucleosynthesis computation. The axes  $[X]$  and  $[\text{Fe}]$  give logarithmic abundances relative to solar for individual elements and for iron, respectively. Solid lines are abundances given by our simulation, which include four metallicities  $z = 0.0001, 0.004, 0.008$  and  $0.02$ . The asterisks correspond to the solar composition, while the dashed diagonal lines intersecting the solar value are the abundances expected if the solar values were scaled with metallicity.

lation. This enrichment of  $^{12}\text{C}$  results in a very high ratio of  $^{12}\text{C}/^{13}\text{C}$ . The total carbon, including  $^{12}\text{C}$  and  $^{13}\text{C}$ , shows an abundance similar to the observation in Fig. 2.

**Nitrogen** is enriched in the great majority of EHe and R CrB stars. Heber (1983) and subsequent authors point out that the N abundances in general follow the trend of the iron abundance. Nitrogen is enriched through CNO cycling in the parent stars. In our simulation, it is subsequently reduced by the  $^{14}\text{N}(\alpha, \gamma)^{18}\text{O}$  reaction

**Oxygen** is enriched in most EHe and R CrB stars. Clayton et al. (2007) report that, for four R CrBs,  $^{18}\text{O}$  has a large enrichment and shows a low ratio of  $^{16}\text{O}/^{18}\text{O}$  close to unity. By comparison with the solar abundance,  $^{18}\text{O}$  must have increased by a factor  $> 400$ . Clayton et al. also indicate that the production of  $^{18}\text{O}$  requires temperatures of at least  $10^8$  K to allow the  $^{14}\text{N}(\alpha, \gamma)^{18}\text{O}$  reaction.  $^{18}\text{O}$  is also produced by  $\alpha$ -capture on  $^{14}\text{N}$  during the fast-accretion phase in our models; the resulting  $^{16}\text{O}/^{18}\text{O}$  ratio is as a function of metallicity, decreasing with  $Z$  (Fig. 3). There is no new  $^{16}\text{O}$  from alpha-capture during the fast-accretion phase.

**Fluorine** is enriched in several EHe stars (Pandey et al. 2006) and in most R CrB stars enriched by factors of 800–8000 relative to its likely initial abundance (Pandey et al. 2008). In our simulation,  $^{19}\text{F}$  comes from reaction of  $^{14}\text{N}(\alpha, \gamma)^{18}\text{F}(p, \alpha)^{15}\text{O}(\alpha, \gamma)^{19}\text{Ne}(\beta^+)^{19}\text{F}$ . Our simulation shows a strong overabundance of F, but not enough to fully agree with the observational data.

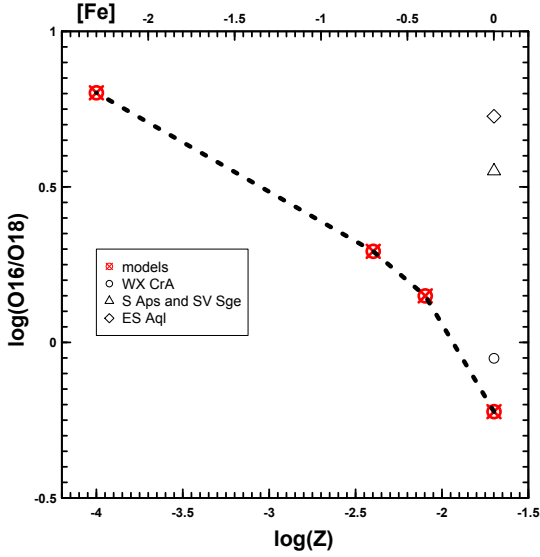


**Figure 3.** The ratio of  $^{16}\text{O}/^{18}\text{O}$  as a function of metallicity. The computation results are shown as circles with crosses. Diamond, triangle and circle symbols show the observations of four  $^{18}\text{O}$  enriched RCrB stars, i.e. WX CrA, S Aps, SV Sge and ES Aql (Clayton et al. 2007).

**Neon.** A high overabundance of neon has been identified in several EHes and RCrBs. In our simulation,  $^{22}\text{Ne}$  is enriched by two  $\alpha$ -captures on  $^{14}\text{N}$  followed by extensive convective mixing.

**Lithium.** A few RCrB stars have a notably large overabundance of lithium, which has so far been difficult to explain. There is no significant lithium produced in our simulation. Longland et al. (2012) indicate that lithium can be produced by the merging of a helium white dwarf with a carbon-oxygen white dwarf if their chemical composition is rich in  $^3\text{He}$  from the previous evolution. This model requires enough  $^3\text{He}$  to be left in the white dwarf after the end of main-sequence evolution and a hot enough corona to form during the merger. As a test calculation, we put  $10^{-5}$  mass fraction of  $^3\text{He}$  into the accreted material, and obtained a surface with a lithium mass fraction of  $1.5 \times 10^{-5}$ , or about  $10^5 \times$  solar. Hence it is clear that if sufficient  $^3\text{He}$  is present in the accreted helium, He+He white dwarf mergers can also yield lithium. Precisely how much depends on many factors, not least the quantity of  $^3\text{He}$  in the donor and the temperature history of the fast-accretion phase.

### 3.3 Some Statistics

The merger frequency of double helium WD systems in the Galaxy is estimated to lie in the range  $0.0057\text{yr}^{-1}$  (Han 1998) (Model 4) to  $0.029\text{yr}^{-1}$  (Webbink 1984). Han (1998) (Fig. 6) shows the final masses of double helium WD mergers to lie roughly in a normal distribution with a mean of  $0.61 \pm 0.09 M_{\odot}$ . Approximately  $\approx 2.3\%$  have a merged total mass  $> 0.8 M_{\odot}$ . Thus, the rate for these high-mass mergers should lie in the range  $1.3 - 6.67 \times 10^{-4} \text{yr}^{-1}$ .

Known low-luminosity helium stars have effective tem-

**Table 1.** Post-merger models with  $4.3 \leq \log T_{\text{eff}} \leq 4.5$ .

Stage	$\log L/L_{\odot}$	Timescale (yrs)	Numbers
A	2.7 – 3	$6 \times 10^4$	8 – 41
B	3.6 – 3.7	$8.6 \times 10^4$	11 – 57
C	4	$2 \times 10^4$	3 – 13

peratures in the range  $4.3 \leq \log T_{\text{eff}} \leq 4.5$  (Jeffery et al. 1996). Considering the evolution tracks through this temperature range, we list the luminosity range and evolution timescales for three different stages of evolution in Table 1 (see also Fig. 1). Combining the evolution time and estimates for the merger frequency, we estimate the number of low-luminosity helium stars in the Galaxy to be  $\approx 8 - 41$  in the inwards-burning phase (stage A),  $\approx 11 - 57$  in the outwards-burning phase (stage B) and  $\approx 3 - 13$  cooling to the white dwarf phase (stage C). Taking the luminosities into account, the *relative* numbers of massive double-WD mergers observable as EHe stars in each stage (A:B:C) should be  $\approx 1 : 6 : 4$ , strongly favouring the post-core-burning stages.

RCrB stars generally have effective temperatures less than 10000K. In the immediate post-merger phase, our He+He merger models with  $T_{\text{eff}} < 10000\text{K}$  have a lifetime of  $\approx 6.7 \times 10^4\text{yrs}$  and a luminosity  $\approx 3$  dex above solar. On the post-subdwarf giant branch they have an equivalent lifetime  $\approx 1.4 \times 10^4\text{yrs}$  and a luminosity  $\approx 4$  dex above solar. Thus, we can estimate the Galactic population to be  $\approx 9 - 43$  newborn hydrogen-deficient giants from massive He+He WD mergers, and  $\approx 2 - 9$  more luminous hydrogen-deficient giants from post-core-burning He-sdO stars. Assuming no intrinsic extinction, the relative numbers of observable cool H-deficient giants in each phase from this channel should be  $\approx 1 : 3$ .

Finally, if we assume a rate of  $0.018 - 0.019\text{yr}^{-1}$  for the merger of CO+He white dwarfs (Webbink 1984; Han 1998), and a mean evolution timescale which is shorter by a factor of 2 due to their higher masses, there would be  $\approx 14 - 70$  times as many RCrB stars from the CO+He merger channel as from the massive He+He channel.

## 4 CONCLUSION

Mergers of helium and carbon-oxygen white dwarfs are currently regarded to be the most favoured model for the origin of most RCrB and EHe stars. The merger of two helium white dwarfs has been widely considered responsible for the origin of some hot subdwarfs, particularly those with hydrogen-deficient surfaces. In this paper we have demonstrated that the most massive helium+helium white dwarf mergers can produce hot subdwarfs which subsequently become cool supergiants and, consequently, provide an alternative means to produce low-mass RCrB and EHe stars. However, the number of RCrB stars produced in this way may be some 14 to 70 times smaller than from the CO+He WD merger channel. Nucleosynthesis of elements during the hot (fast-accretion) phase of the merger is roughly consistent with the observed abundances of  $^{12}\text{C}$ ,  $^{18}\text{O}$ ,  $^{19}\text{F}$  and  $^{22}\text{Ne}$  in RCrB and EHe stars. Further work is required to establish whether the products of massive He+He WD mergers

can be clearly distinguished from the products of CO+WD mergers.

## ACKNOWLEDGMENTS

The Armagh Observatory is supported by a grant from the Northern Ireland Dept. of Culture Arts and Leisure.

## REFERENCES

- Benz W., Cameron A. G. W., Press W. H., Bowers R. L., 1990, *ApJ*, 348, 647
- Brown J. M., Kilic M., Brown W. R., Kenyon S. J., 2011, *ApJ*, 730, 67
- Clayton G. C., Geballe T. R., Herwig F., Fryer C., Asplund M., 2007, *ApJ*, 662, 1220
- Clayton G. C., Sugerman B. E. K., Stanford S. A., Whitney B. A., Honor J., 2011, *ApJ*, 743, 44
- Cropper M., Harrop-Allin M. K., Mason K. O., Mittaz J. P. D., Potter S. B., Ramsay G., 1998, *MNRAS*, 293, L57
- Dinger A. S., 1972, *MNRAS*, 158, 383
- Evans C. R., Iben Jr. I., Smarr L., 1987, *ApJ*, 323, 129
- Guerrero J., García-Berro E., Isern J., 2004, *A&A*, 413, 257
- Han Z., 1998, *MNRAS*, 296, 1019
- Hirsch H., 2009, PhD thesis, University of Erlangen-Nürnberg
- Iben I., Renzini A., 1984, *Physics Reports*, 105, 329
- Jeffery C. S., Heber U., Hill P. W., Dreizler S., Drilling J. S., Lawson W. A., Leuenhagen U., Werner K., 1996, in C. S. Jeffery & U. Heber ed., *Hydrogen Deficient Stars* Vol. 96 of *Astronomical Society of the Pacific Conference Series*, A catalogue of hydrogen-deficient stars. pp 471–480
- Jeffery C. S., Karakas A. I., Saio H., 2011, *MNRAS*, 414, 3599
- Kilic M., Brown W. R., Allende Prieto C., Agüeros M. A., Heinke C., Kenyon S. J., 2011, *ApJ*, 727, 3
- Kilic M., Brown W. R., Allende Prieto C., Kenyon S. J., Panei J. A., 2010, *ApJ*, 716, 122
- Longland R., Lorén-Aguilar P., José J., García-Berro E., Althaus L. G., 2012, *ArXiv e-prints*
- Longland R., Lorén-Aguilar P., José J., García-Berro E., Althaus L. G., Isern J., 2011, *ApJL*, 737, L34
- Lorén-Aguilar P., Isern J., García-Berro E., 2009, *A&A*, 500, 1193
- Nelemans G., Verbunt F., Yungelson L. R., Portegies Zwart S. F., 2000, *A&A*, 360, 1011
- Nelemans G., Yungelson L. R., Portegies Zwart S. F., Verbunt F., 2001, *A&A*, 365, 491
- Paczyński B., 1971, *Acta Astronomica*, 21, 1
- Pakmor R., Hachinger S., Röpke F. K., Hillebrandt W., 2011, *A&A*, 528, A117
- Pandey G., Lambert D. L., Jeffery C. S., Rao N. K., 2006, *ApJ*, 638, 454
- Pandey G., Lambert D. L., Rao N. K., 2008, *ApJ*, 674, 1068
- Paxton B., Bildsten L., Dotter A., Herwig F., Lesaffre P., Timmes F., 2011, *ApJS*, 192, 3
- Rebassa-Mansergas A., Nebot Gómez-Morán A., Schreiber M. R., Girven J., Gänsicke B. T., 2011, *MNRAS*, 413, 1121
- Saio H., Jeffery C. S., 2000, *MNRAS*, 313, 671
- Saio H., Jeffery C. S., 2002, *MNRAS*, 333, 121
- Trimble V., Paczynski B., 1973, *A&A*, 22, 9
- Warner B., 1967, *MNRAS*, 137, 119
- Webbink R. F., 1984, *ApJ*, 277, 355
- Weiss A., 1987, *A&A*, 185, 165
- Yoon S., Podsiadlowski P., Rosswog S., 2007, *MNRAS*, 380, 933
- Zhang X., Jeffery C. S., 2012, *MNRAS*, 419, 452